

Kinematic Orbit Determination of Low Earth Orbiting Satellites using GPS Observables

Muhammad Zaheer

Abstract— Global positioning system (GPS) observables can be used to compute the orbits of low earth orbiting (LEO) satellites using kinematic approach. Data from GPS receiver, installed onboard the LEO satellite is used for this purpose.

In present paper, GPS data from challenging Mini-satellite Payload (CHAMP) is used for its orbit determination. The ionospheric effects on GPS raw data are removed by frequency combination technique. Furthermore, the CHAMP orbit computed using the GPS data are compared with jet propulsion laboratory's (JPL) published CHAMP spacecraft orbit for same epochs. The root mean square difference in Earth centered Earth fixed (ECEF) Coordinates and JPL computed coordinates are compared. The standard deviations of the differences in ECEF coordinates (JPL results – GPS computed results) is presented. CHAMP orbits computed by JPL have accuracy of centimeter level. Therefore the difference in results of GPS data computed orbits and JPL computed orbits can also be referred as observed error in our method. On this basis, accuracy of our method is analyzed. The observed standard deviation of difference/errors is about 11m.

Index Terms— ambiguity integer, ambiguity resolution; code observable; Kalman filter; phase observable.

I. INTRODUCTION

Satellites in space frequently undergo thrust and other perturbations which disturb their orbits continuously.

Therefore, it is essential to keep predicting their motion and perform orbit determination on them to meet the desired mission life. For this purpose, researchers have always been trying to find some ways to improve orbit determination including use of new estimation techniques. Jerome has presented fifty years history of satellite orbit determination in [6]. Employment of GPS observables for orbit determination is one of the modern techniques being used today. Improved accuracy of GPS observables also promises their future use in attitude determination of satellites as presented in [12]

Orbits of low earth orbiting (LEO) satellites can be determined using kinematic technique. Code and phase observables for L1 and L2 frequencies of GPS are recorded to compute the LEO satellite orbit. During the last two decades, several LEO missions have been equipped with a GPS receiver (like CHAMP or GRACE etc). Precise orbit determination of these missions has shown that GPS data based orbit determination with good accuracy is possible. Data from these missions can be used to analyze the developed algorithm for orbit determination. Several algorithms are available for GPS positioning like, [3] have presented a

recursive least squares algorithm for GPS data based positioning using carrier phase and code measurements.

Andersson in [1] and [2] has used undifferenced approach of GPS positioning to develop a complete displacement monitoring system during his doctoral studies. This algorithm can be modified easily to compute the satellite orbits. The ionospheric effects can be removed according to the method presented by Sjöberg and Horemuž in [10].

The author, during his masters' degree thesis work, in [11] has derived necessary mathematical equations and models required for computing the satellite orbit. Here equations for code pseudoranges and phase observables are discussed briefly.

A. The code pseudorange observable

GPS signals travel with the speed of light therefore, by knowing the travelling time from satellite to receiver, the distance from satellite to receiver can be computed using equation

$$P_A^S(t_A) = (t_A - t^s)c \quad (1)$$

where t_A represents nominal receiver time at which signal is received at receiver, t^s represents time when signal is emitted by GPS satellite and c is speed of light.

Equation (1) does not include the clock biases, therefore we introduce these biases and finally resultant distance equation is linearized to obtain pseudorange observation equation

$$P_A^S(t_A^*) = \rho_A^S(t_A) + \dot{\rho}_A^S(t_A)\delta t_A - \delta t^s c \quad (2)$$

B. The phase observable

The GPS receiver generates the carrier phase at the signal reception time and the same is compared with phase of the received satellite signal to measure the phase observable. Phase observable is defined as measure of the phase of the received GPS satellite signal relative to the carrier phase generated by receiver at reception time. This can be measured by shifting the receiver-generated phase and further tracking the received phase. The phase observation equation is derived by the author in [11] and is given by

$$\Phi_A^S(t_A) = \rho_A^S(t_A) + (\dot{\rho}_A^S(t_A) + c)\delta t_A - c\delta t^s + \lambda N_A^S \quad (3)$$

Where λ represents wavelength of the signal and N is unknown integer ambiguity.

There are some biases and noises which can be related to satellite, the propagation media and the receiver as divided by Hoffman-Wellenhof in [5] in to these three groups. These biases and noises are not included in equation (3). Therefore some additional terms will also be included in equation (3) to model the systematic errors. These terms are listed in Table I

TABLE I. ADDITIONAL BIASES TO GPS SIGNAL [1]

Receiver	$\delta M_{A,i}^S$	Multipath Error
	δt_A	Receiver clock offset
	$\delta H_{A,i}$	Hardware delay bias of receiver
	$\delta A_{A,i}^S$	Antenna phase centre variations
Media	I_A^S	Ionospheric delay
	T_A^S	Zenith Tropospheric delay
Satellite	δO_A^S	Orbital errors
	δt^S	Satellite clock offset
	δH_i^S	Hardware delay bias of satellite
	δA_i^S	Antenna offset of satellite
	T_{GD}^S	Satellite Code offset

The subscript A and superscript S depict the relevance of the bias to satellite, receiver or both. Index “i” is either L1 or L2 which shows that the variable is frequency dependant.

Hardware errors in the satellite like δH_i^S often assumed to be zero because they cannot be separated from clock offset [1]. Time offset between C1 and P2 code message T_{GD}^S and is inseparable from the receiver hardware delay. It can be used by dual frequency users to eliminate the ionospheric effects conventionally at the receiver end.

The terms related to atmospheric errors, listed in Table I, depend upon actual condition of the ionosphere and atmosphere along the path through which the signal propagates.

Multipath effect at receiver antenna is dictated by actual environment around it because this effect is caused by the reflecting surface reflected signal collected by receiver. It can be removed for static surveys having long time of observations; however this effect is significant for rapid surveys. According to [5], it can grow as large as 100m in when observations are taken near buildings or other special environments.

Dedes and Mallett have analyzed the effects of ionosphere on long baseline GPS positioning [4]. I have used ambiguity resolution technique presented by Sjöberg and Horemuž in [10]. This technique uses combination of phase and code

observables to introduce an ionofree observable for position computation.

The actual phase centre of antenna is slightly different from its geometrical centre, therefore this phenomenon gives rise to phase centre variations denoted by $\delta A_{A,i}^S$. It has to be dealt with considering antenna calibration data.

Adding all these terms to equations (2) and (3), these equations are reshaped as [11]

$$P_{A,1}^S(t_A) = \rho_A^S(t_A) + (\dot{\rho}_A^S + c)\delta t_A - c(\delta t^S - T_{GD}^S) + I_A^S(t_A) + m_A^S T_A(t_A) + \delta O_A^S(t_A) + \delta M_{A,P1}^S(t_A) + \delta H_{A,P1}(t_A) + \delta H_{P1}^S(t_A) + \delta A_{A,P1}^S(t_A) + \delta A_{P1}^S(t_A) + \varepsilon_{P1} \quad (4)$$

$$P_{A,2}^S(t_A) = \rho_A^S(t_A) + (\dot{\rho}_A^S + c)\delta t_A - c(\delta t^S - T_{GD}^S) + I_A^S(t_A) + m_A^S T_A(t_A) + \delta O_A^S(t_A) + \delta M_{A,P2}^S(t_A) + \delta H_{A,P2}(t_A) + \delta H_{P2}^S(t_A) + \delta A_{A,P2}^S(t_A) + \delta A_{P2}^S(t_A) + \varepsilon_{P2} \quad (5)$$

and

$$\Phi_{A,1}^S(t_A) = \rho_A^S(t_A) + (\dot{\rho}_A^S + c)\delta t_A - c(\delta t^S) + \lambda_{L1} N_{A,L1}^S - I_A^S(t_A) + m_A^S T_A(t_A) + \delta O_A^S(t_A) + \delta M_{A,L1}^S(t_A) + \delta H_{A,L1}(t_A) + \delta H_{L1}^S(t_A) + \delta A_{A,L1}^S(t_A) + \delta A_{L1}^S(t_A) + \varepsilon_{L1} \quad (6)$$

$$\Phi_{A,2}^S(t_A) = \rho_A^S(t_A) + (\dot{\rho}_A^S + c)\delta t_A - c(\delta t^S) + \lambda_{L2} N_{A,L2}^S - \alpha_f I_A^S(t_A) + m_A^S T_A(t_A) + \delta O_A^S(t_A) + \delta M_{A,L2}^S(t_A) + \delta H_{A,L2}(t_A) + \delta H_{L2}^S(t_A) + \delta A_{A,L2}^S(t_A) + \delta A_{L2}^S(t_A) + \varepsilon_{L2} \quad (7)$$

Since measurements contain random noises therefore the terms ε_{P1} , ε_{P2} , ε_{L1} and ε_{L2} are added in the end of equations (4) to (6) respectively and their values are listed by Hoffman-Wellenhof in [5].

B. The positioning methods and state vector models

Different positioning methods like single difference method, double difference method and triple difference methods are

used which are listed in [7]. We have used undifferenced method, which is an alternate to double difference method. This method can avoid the singularity introduced due to the ionospheric and hardware delays of the phase observations. Therefore least square solution (LSQ) would not be singular when we use this method.

The real challenge with undifferenced method is to model the real time correlation between measurements of epochs after which, Kalman filter can estimate the unknowns for each epoch. Complete derivation of state vector model for undifferenced solution is carried out by the author in [11]. For position and velocity estimation, velocity is assumed to be constant. This assumption enables us to model the velocity as random walk process. The state vector of receiver is given by

$$X_{PV,A} = [X_A \ v_A]^T = [X_A \ Y_A \ Z_A \ v_{xA} \ v_{yA} \ v_{zA}]^T \quad (8)$$

with,

$$\begin{cases} \dot{X}_A = v_A \\ \dot{v}_A = u_a \end{cases} \quad (9)$$

and

$$E[u_a(s)u_a^T(t)] = Q_A = \begin{bmatrix} q_{AX} & 0 & 0 \\ 0 & q_{AY} & 0 \\ 0 & 0 & q_{AZ} \end{bmatrix} \quad (10)$$

are dynamic model and covariance matrix respectively.

Where q_{AX} , q_{AY} & q_{AZ} are the power powers spectral densities (PSD) of the acceleration having units $(m^2/S^4) / Hz$.

The dynamic matrix $F_{PV,A}$, gain coefficients matrix $G_{PV,A}$ and random noise force function $u_{a,A}$ are

$$F_{PV,A} = \begin{bmatrix} 0 & 0 & 0 & 1 & 0 & 0 \\ 0 & 0 & 0 & 0 & 1 & 0 \\ 0 & 0 & 0 & 0 & 0 & 1 \\ 0 & 0 & 0 & 0 & 0 & 0 \\ 0 & 0 & 0 & 0 & 0 & 0 \\ 0 & 0 & 0 & 0 & 0 & 0 \end{bmatrix}, G_{PV,A} = \begin{bmatrix} 0 & 0 & 0 \\ 0 & 0 & 0 \\ 0 & 0 & 0 \\ 1 & 0 & 0 \\ 0 & 1 & 0 \\ 0 & 0 & 1 \end{bmatrix} \quad (11)$$

and

$$u_{a,A} = \begin{bmatrix} u_{aX} \\ u_{aY} \\ u_{aZ} \end{bmatrix}$$

The process noise covariance matrix becomes (for $F^n = 0$, $n \geq 2$):

$$Q_A = Q_G \Delta t + (F Q_G + Q_G F^T) \frac{\Delta t^2}{2} + F Q_G F^T \frac{\Delta t^3}{3} \quad (12)$$

with

$$Q_A = \begin{bmatrix} \left(\frac{q_{ax}\Delta t^3}{3}\right) & 0 & 0 & \left(\frac{q_{ax}\Delta t^2}{2}\right) & 0 & 0 \\ 0 & \left(\frac{q_{ay}\Delta t^3}{3}\right) & 0 & 0 & \left(\frac{q_{ay}\Delta t^2}{2}\right) & 0 \\ 0 & 0 & \left(\frac{q_{az}\Delta t^3}{3}\right) & 0 & 0 & \left(\frac{q_{az}\Delta t^2}{2}\right) \\ \left(\frac{q_{ax}\Delta t^2}{2}\right) & 0 & 0 & q_{ax}\Delta t & 0 & 0 \\ 0 & \left(\frac{q_{ay}\Delta t^2}{2}\right) & 0 & 0 & q_{ay}\Delta t & 0 \\ 0 & 0 & \left(\frac{q_{az}\Delta t^2}{2}\right) & 0 & 0 & q_{az}\Delta t \end{bmatrix} \quad (13)$$

The transition matrix is

$$T_{PV,A} = I + F_{PV,A} \Delta t = \begin{bmatrix} 1 & 0 & 0 & \Delta t & 0 & 0 \\ 0 & 1 & 0 & 0 & \Delta t & 0 \\ 0 & 0 & 1 & 0 & 0 & \Delta t \\ 0 & 0 & 0 & 1 & 0 & 0 \\ 0 & 0 & 0 & 0 & 1 & 0 \\ 0 & 0 & 0 & 0 & 0 & 1 \end{bmatrix} \quad (14)$$

Ionosphere and troposphere have their effects on the signal propagation however here we have to deal only with ionosphere because the ionospheric height is about 50km from mean sea level (MSL) which is far less than the altitude of the CHAMP spacecraft (whose data is used for orbit determination)

To remove the ionospheric effect, we have used linear combination of the phase and code observables, a method presented by Sjöberg and Horemuz in [10]. An artificial ionospheric observable is used for this purpose which has zero observed value and certain variance. Based on this, the double difference ambiguities for each satellite are estimated employing smoothed pseudoranges and combination of phases.

Let we have two phase observations with phases Φ_1 and Φ_2 having ambiguities N_1 and N_2 respectively. This method says that it is better to formulate the liner combination of N_1 and N_2 $N_{ij} = iN_1 + jN_2$ instead of estimating them separately.

Following equation is used for this linear combination

$$\Phi_{ij} = \rho + \lambda_{ij} N_{ij} \quad (15)$$

where,

$$\Phi_{ij} = \left(i \frac{\Phi_1}{\lambda_1} + j \frac{\Phi_2}{\lambda_2} \right) \quad \text{and} \quad \lambda_{ij} = \left(\frac{i}{\lambda_1} + \frac{j}{\lambda_2} \right)^{-1} \quad (16)$$

We have combined the L_1 and L_2 phases and applied single point positioning, coordinates and velocities of the receiver are computed.

Other errors like receiver antenna phase centre difference, receiver clock offsets, common errors and multipath errors are discussed in [1].

C. The observation equations

Considering all parameters discussed in previous heading, equations (4) to (7) can be re-written as code and phase observation equations.

1. The code observation equation

Code observation equations for L1 and L2 are given as

$$\begin{aligned} \delta P_{A,1}^S(t_A) &= (\dot{\rho}_A^S + c)\delta t_A + I_A^S(t_A) + \\ & m_{w,A}^S T_{w,A}(t_A) + \delta O_A^S(t_A) + \varepsilon_{P1} \end{aligned} \quad (17)$$

and

$$\begin{aligned} \delta P_{A,2}^S(t_A) &= (\dot{\rho}_A^S + c)\delta t_A + \alpha_f I_A^S(t_A) + \\ & m_{w,A}^S T_{w,A}(t_A) + \delta O_A^S(t_A) + \varepsilon_{P2} \end{aligned} \quad (18)$$

2. The phase observation equation

Similarly phase observation equation, after including all parameters, become

$$\begin{aligned} \delta \Phi_{A,1}^S(t_A) &= (\dot{\rho}_A^S + c)\delta t_A + \lambda_{L1} N_{A,L1}^S - I_A^S(t_A) \\ & + m_{w,A}^S T_{w,A}(t_A) + \delta O_A^S(t_A) + \varepsilon_{L1} \end{aligned} \quad (19)$$

and

$$\begin{aligned} \delta \Phi_{A,2}^S(t_A) &= (\dot{\rho}_A^S + c)\delta t_A + \lambda_{L2} N_{A,L2}^S - \alpha_f I_A^S(t_A) \\ & + m_{w,A}^S T_{w,A}(t_A) + \delta O_A^S(t_A) + \varepsilon_{L2} \end{aligned} \quad (20)$$

LHS of above equations (17) to (20) represent the deterministic parameters and RHS have stochastic parameters to be estimated using Kalman filter. The author has discussed all of these parameters in [11].

D. The Kalman filter implementation

The detail derivation and application process of Kalman filter is given in [11], here we just summarize its three steps; the prediction, gain calculation and update step. We need to initialize the filter with somehow known set of initial values of the state vector so that the filter does not diverge [1]. The

initialization is followed by the prediction step, where parameters are predicted from the previous epoch to the current epoch which is given by following two equations

$$\hat{X}_k^- = T_{k,k-1} \hat{X}_{k-1} \quad (21)$$

and

$$Q_{X,k}^- = T_{k,k-1} Q_{X,k-1} T_{k,k-1}^T + Q_k \quad (22)$$

where superscript “-” symbolizes a predicted and “^” an estimated parameter.

The next step of the filter is gain calculation which is carried out according to following equation

$$K_k = Q_{X,k}^- H_k^T [R_k + H_k Q_{X,k}^- H_k^T]^{-1} \quad (23)$$

The last recursive step of the filter is update step carried out using following equation

$$\hat{X}_k = \hat{X}_k^- + K_k (L_k H_k \hat{X}_k^-) \quad (24)$$

The covariance matrix can be updated using following equation

$$Q_{X,k} = (I - K_k H_k) Q_{X,k}^- (I - K_k H_k)^T + K_k R_k K_k^T \quad (25)$$

Each recursive loop of Kalman filter uses equations (21) to (25).

E. The software implementation

The software consists of different MATLAB codes which are integrated together for post processing of GPS data. Kalman filter algorithm developed by Andersson [1] is integrated with some sub-modules. The author has modified this algorithm/software according to the needs for computation of CHAMP orbit. Undifferenced approach of GPS based positioning is used. Kalman filter output gives estimated parameters of the state vector and their standard deviations. Software functional steps are summarized in Figure 1.

In the first step software is initialized and then it moves to next step. Till the end of input data, the Kalman filter algorithm keeps itself repeating. At the output we get estimated parameters and standard deviations. The state vector at output of Kalman filter contains the computed X, Y and Z coordinates and velocities in ECEF frame. Necessary equations for conversion to geodetic coordinates are given by Ligan in [8]. All of these steps are explained in detail by the author in [11].

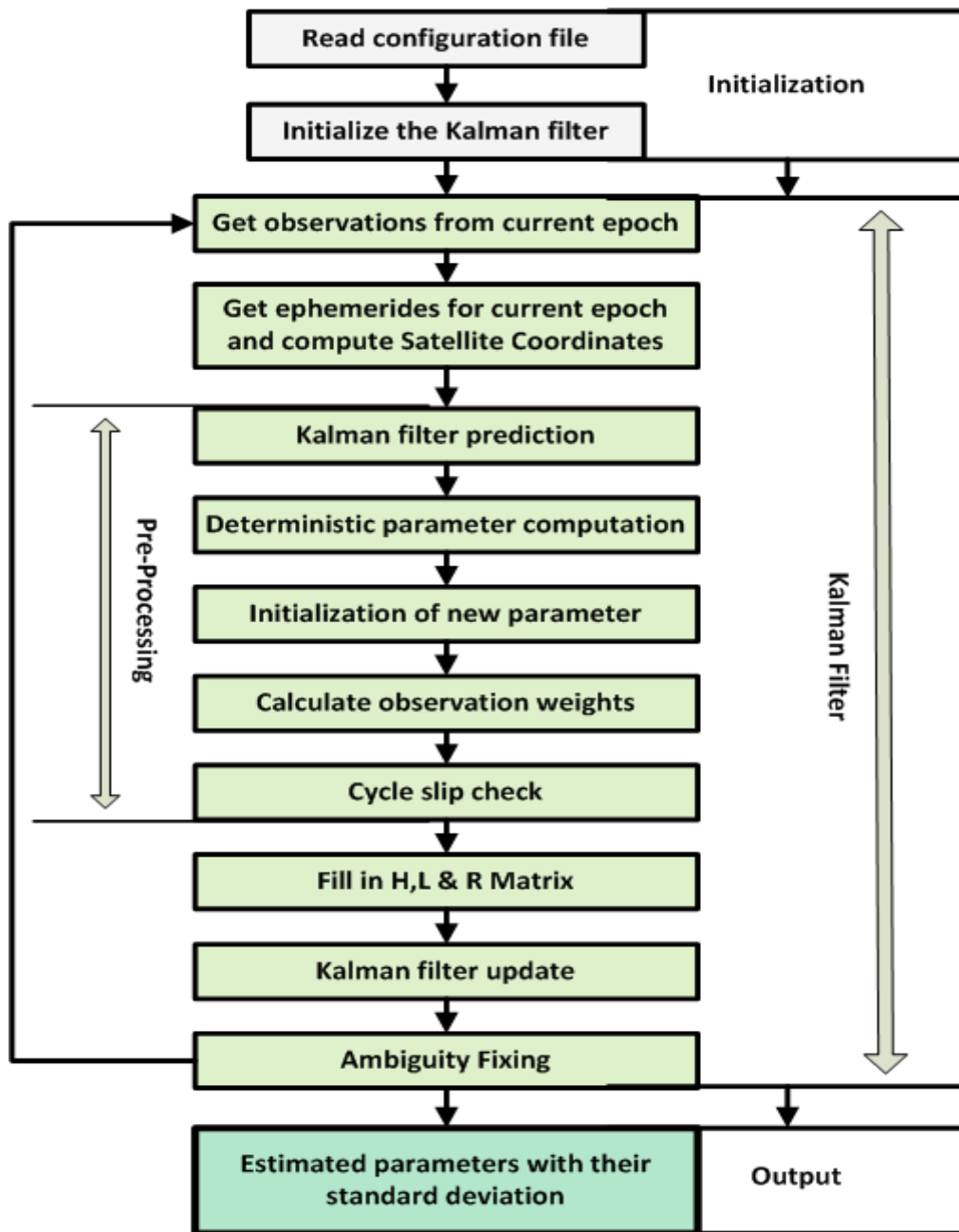


Figure 1 Functional and implementation steps of software

1) The initialization step

In initialization step, the software reads the configuration file that dictates different future decisions (like single frequency computation or double frequency computation, minimum and maximum acceptable elevation angle of satellite, etc) and it also contains some initial values and file names (e.g. precise/broadcast ephemeris file name, navigation data file name etc). The next step is pre-processing during which Kalman filter is predicted, deterministic parameters are computed, new parameters are initialized and observation weights are computed to detect the cycle slip.

1. Computation of satellite orbits

Satellite positions are computed using precise ephemerides by interpolation technique using following polynomial

$$p(t) = a_1 t^n + a_2 t^{n-1} + \dots + a_n t + a_{n+1} \quad (26)$$

The general flow chart for computation of satellite orbits using precise ephemerides (PE) or broadcast ephemerides (BE) is given in Figure 2.

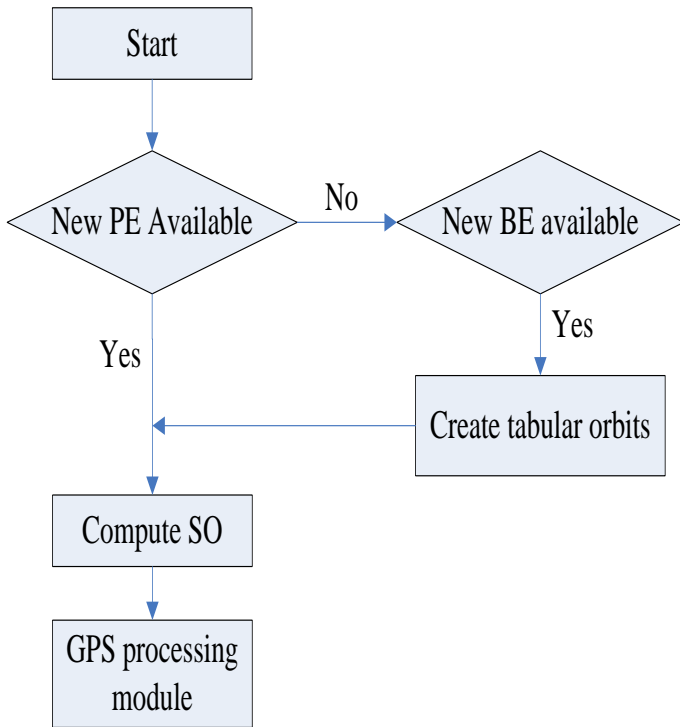


Figure 2 General flowchart for computing satellite positions [1]

2. Observations weighing

The GPS signal has to travel through ionosphere and troposphere therefore noise level may be different for signals received from different GPS satellites available at particular elevation angle. To deal with this problem, observation weighing is used. Following equation is used for observation weighing purpose

$$\sigma_E^2 = \frac{a_0^2}{\sin^2 E} \quad (27)$$

E is elevation angle towards GPS satellite and a_0 is empirically estimated coefficient, σ_E^2 is a-priori variance for the variance-covariance matrix R and it can be computed when a_0 is known.

3. Cycle slip detection

After this step the software detects the cycle slips. Many methods are available for this purpose. We have used single frequency phase /code combination and dual frequency phase combination. Detail of these methods is available in [11].

4. Filling in H , L and R matrix

In the next step the software fills in the design matrix H , observation vector L and the variance-covariance matrix R for each of the recursive loop of Kalman filter.

5. Ambiguity fixing

Lambda method is used for ambiguity fixing. We provide ambiguity the parameters in the state vector X_k and the corresponding part of covariance matrix Q_x at the input of this algorithm. This algorithm returns two alternative solutions for the ambiguities. We control the ratio between them by the following equation given in [7] at page 371.

$$\frac{\min_{2nd\ best}}{\min_{best}} > 3 \quad (28)$$

The ambiguity is fixed when condition in above equation is met. If the condition is not met, it is kept unfixed until the next loop of the algorithm.

6. Output parameters

At the output of the Kalman filter we get estimated parameters of the state vector X along with standard deviations which are further. We can also get

- Cycle slip detection parameters for single-frequency, iono-free and geometry-free combinations.
- Number of satellites at each receiver.
- The residuals for each observation type
($v = (\tilde{L} - h(\hat{X}))$)
- The predicted residuals for each observation type
($v = (\tilde{L} - h(\hat{X}^-))$)

II. RESULTS AND DISCUSSIONS

A. Available data

GPS data (pseudoranges and phase observables) from CHAMP satellite, for the epoch day/time (01-01-2002)/00.00h to (02-01-2002)/00.00h was used to compute the CHAMP orbit. This data corresponds to CHAMP orbits number 8247 and onwards. To avoid the long computational time, this data was divided into time intervals corresponding to CHAMP periods and tagged according to the orbit number/revolution numbers.

B. Orbit computation and results analysis

Using data, discussed in section II-A and the mathematical models discussed in preceding sections, we computed the orbit for four periods of CHAMP starting from orbit number 8247 till orbit number 8250 for the epoch day (01-01-2002). The results are quite promising. Ground tracks (of orbit number 8247 till 8250) of CHAMP spacecraft are given in Figure 3. Since the result obtained by our algorithm does not diverge, therefore initial functionality of our algorithm is validated by this result.

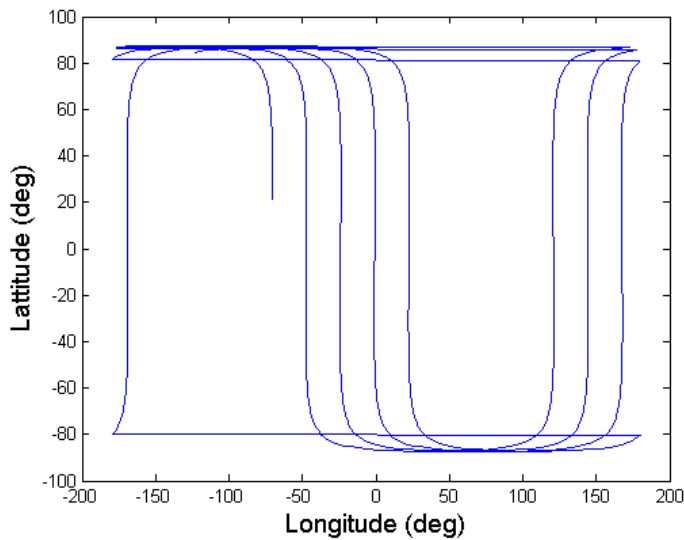


Figure 3 CHAMP satellite ground tracks computed using GPS observables

The residuals of any measurement are most important factor which decides the acceptability of the measurements. Our algorithm computes the residuals for each observation type using the relation $(v = (\tilde{L} - h(\tilde{X}))$. These residuals of P1 and P2 (pseudorange code observations for GPS frequencies L1 and L2) observations are given in Figures 4 and 5. These residuals are mostly below decimeter level, except some spikes which can arise by random noise, therefore we can say that our algorithm is functioning properly and giving good results.

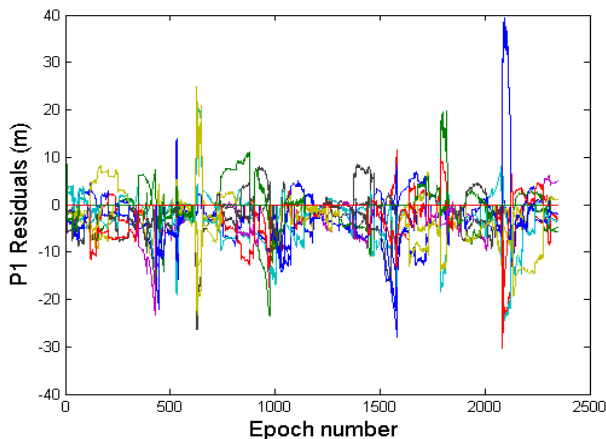


Figure 4 P1 residuals calculated for available GPS satellite

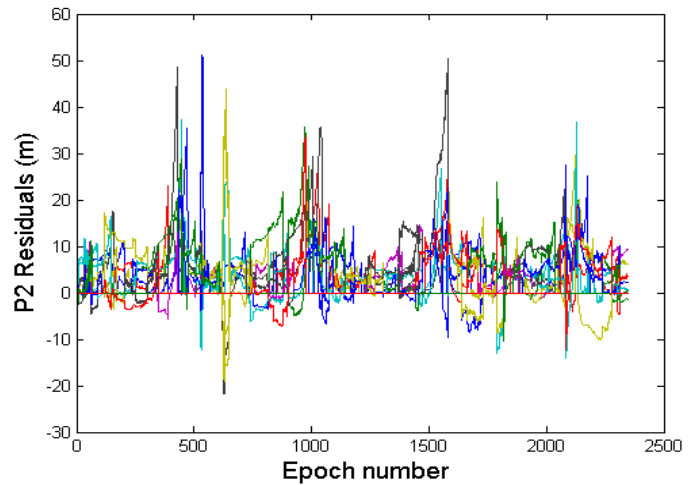


Figure 5 P2 residuals calculated for available GPS satellite

Standard deviation of ECEF X, Y and Z coordinates, computed using GPS observables is given in Figure 6 and is mostly below 0.5 meters. However some spikes are observed due to random noise (or maybe due to other factors) up to 2 meters at maximum.

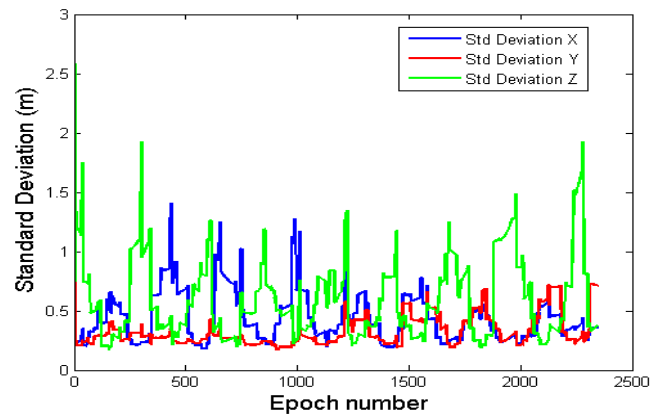


Figure 6 Standard deviations of XYZ coordinates computed using GPS observables

C. Results validation by comparison with JPL computed CHAMP orbits

Orbit data of CHAMP spacecraft, computed by JPL (<ftp://sayatnova.jpl.nasa.gov/pub/genesis/orbits/champ/>) was used as reference to estimate the accuracy of our algorithm. These orbits for the CHAMP spacecraft were created for JPL's rapid processing of CHAMP GPS data using GIPSY/OASIS II software. This software is precise up to centimeter-level for GNSS-based positioning (<https://gipsy-oasis.jpl.nasa.gov/>). Further details of orbit determination strategy are available at <ftp://sayatnova.jpl.nasa.gov/pub/genesis/orbits/champ/quick/DOCUMENTS/README.quick>.

A comparison of the ECEF X, Y and Z coordinates, computed by using GPS data and JPL published data is shown in following Figures 7 to 9.

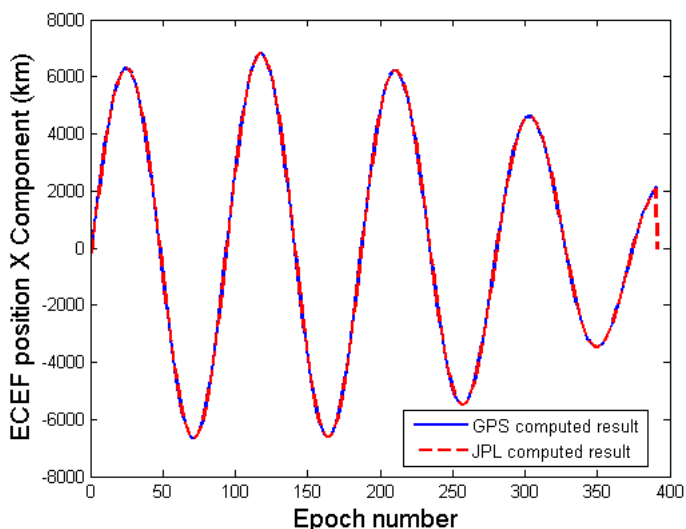


Figure 7 ECEF X component of CHAMP computed by GPL and using GPS observables

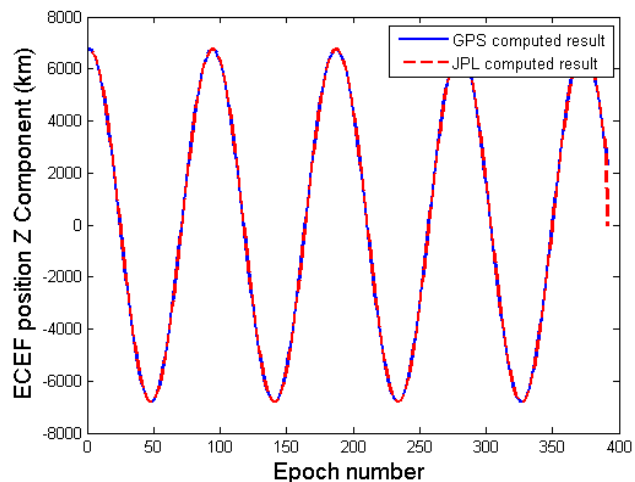


Figure 9 ECEF Z component of CHAMP computed by GPL and using GPS observables

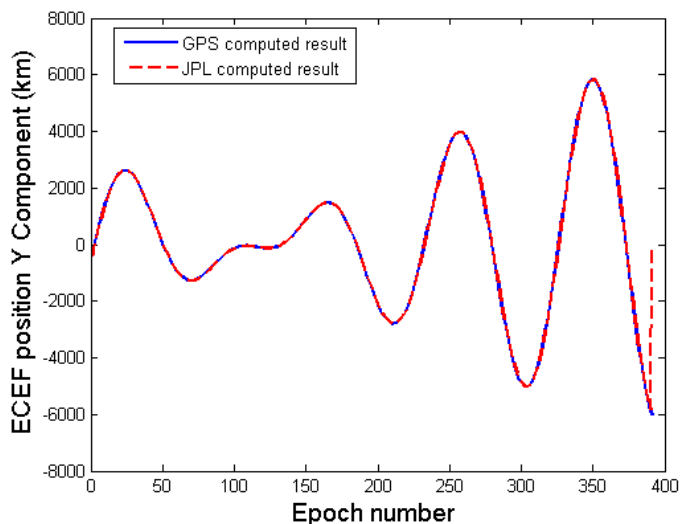


Figure 8 ECEF Y component of CHAMP computed by GPL and using GPS observables

It is very easy to calculate the root mean square (RMS) of the difference (JPL computed positions – GPS data computed positions) in ECEF position X, Y and Z coordinates. RMS difference for ECEF-X coordinate is plotted in Figure 10. Standard deviation of this difference is 11.7m. Therefore we can expect that accuracy of our computed results is within 12m other than some spikes which may occur due to random noise or other factors. These results show that the orbit computed using GPS data are well agreeing to the true orbit of CHAMP spacecraft and our algorithm is functioning properly with good accuracy.

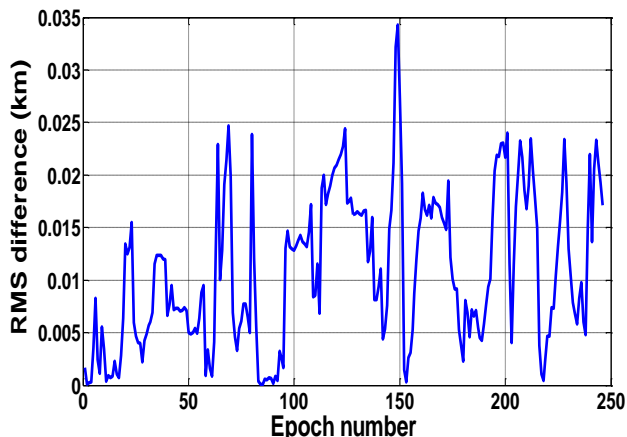


Figure 10 RMS difference (JPL-GPS) of X coordinate

Comparison of results plotted in Figures 7 to 9 shows that the results produced by our algorithm are well agreeing to the precise orbits determined by JPL for CHAMP spacecraft.

III. CONCLUSION

The present paper has presented algorithm to compute LEO satellite orbit using GPS observables which is functioning quite properly. Residuals of P1 and P2 observations are computed, furthermore standard deviations of ECEF-X, Y and Z coordinates are computed and these parameters show that the presented algorithm is fairly accurate for computation of satellite orbits. The accuracy of algorithm is around 11m as compared to JPL's computed CHAMP orbit.

The author [11], during his masters' degree thesis work has compared the results of this algorithm with satellite tool kit (STK) propagated orbits of CHAMP and found that results are in agreement with STK propagated orbits.

In this paper I computed CHAMP orbit with the available data for one day which may be extended for other periods of CHAMP, if data is available. However the trend of residuals and computed standard deviation shows that., the errors will grow for longer time computations therefore this aspect of the presented algorithm needs further studies which can done in future work. A proper algorithm, developed to predict and reduce the random errors will increase the performance of this algorithm while reducing the effect of the random errors on Kalman filter loop. In this regard application of MINQUE method presented by Rao in [9] will be very useful.

ACKNOWLEDGEMENTS

The author is obliged to Dr. Rasheed Ahmed Baloch, Dy. Director General (Quality Management Directorate Gen, SUPARCO) for his guidance and support during this research work.

Most of this research work was carried out during Masters Degree thesis work in School of Architecture and Built Environment, Division of Geodesy and Geo-Informatics, Royal Institute of Technology (KTH) Sweden. The author is also grateful to Dr. Milan Horemuž for his entire help and guidance.

REFERENCES

- [1] Andersson J V, (2006), Undifferenced GPS for deformation monitoring, KTH, Licentiate thesis in Geodesy, Stockholm, ISBN 13:978-91-85539-03-1
- [2] Andersson J. V., (2008), A complete model for displacement monitoring based on undifferenced GPS observations, ISBN ISBN 10: 91-85539-30-9
- [3] Chang X W, Paige C C, Yin L, (2005), Code and carrier phase based short baseline GPS positioning: computational aspects. *GPS Solutions* 9(1): 72-83
- [4] Dedes G, Mallett A, Effects of the Ionosphere and Cycle-Slips In Long Baseline Dynamic Positioning. *Proc. of ION GPS-95*, pp. 1081-1090.
- [5] Hoffmann-Wellenhof B., Lichtenegger H, Collins J, (2001), *GPS Theory and Practice*, Fifth Edition, Springer-Verlag, Wien New York, ISBN 3-211-83534-2
- [6] Jerome V R, Number 3 (2007), Fifty Years of Orbit Determination: Development of Modern Astrodynamics Methods, John S Hopkins APL Technical Digest, Volume 27
- [7] Leick A., (2004), *GPS Satellite Surveying*, Third Edition, John Wiley and Sons, ISBN 0-471-05930-7
- [8] Ligas M, Banasik P, (2011), Conversion between Cartesian and geodetic coordinates on a rotational ellipsoid by solving a system of nonlinear equations, *Polish Academy of Sciences, geodesy and cartography*, Vol. 60
- [9] Rao C R, (1971), Estimation of variance components-MINQUE theory. *J. Multivar. Anal.*, 1, 257-275.
- [10] Sjöberg L. E., Horemuž M., (2002). Rapid GPS ambiguity resolution for short and long baselines, *Journal of Geodesy* (2002) 76:381-391, Royal Institute of Technology, Sweden
- [11] Zaheer M., "Kinematic orbit determination of low Earth orbiting satellites, using satellite-to-satellite tracking data and comparison of results with different propagators," Master of Science Thesis in Geodesy No. 3130 TRITA-GIT EX 14-001, ISSN 1653-5227 , ISRN KTH/GIT/EX--14/001-
- [12] Ziebart M and Cross P, (2003) LEO GPS attitude determination algorithm for a micro-satellite using boom-arm deployed antennas, *GPS Solutions* (2003) 6:242-256